



# The Role of High-order Phase Correlations in Texture Processing

JONATHAN D. VICTOR,\*† MARY M. CONTE\*

Received 27 March 1995; in revised form 31 July 1995

**Isodipole textures are pairs of texture ensembles whose autocorrelations, and hence power spectra, are equal. Examples of readily discriminable isodipole textures are well known. Such discriminations appear to require feature extraction, since the isodipole condition eliminates ensemble differences in spatial frequency content. We studied the effects of phase decorrelation on VEP indices of discrimination of isodipole texture pairs. Phase decorrelation, which ranged from  $0.125\pi$  radians (slight randomization) to  $\pi$  radians (complete randomization), was introduced in two ways: by independent jittering of each spatial Fourier component, and by a product method, which preserved correlations among certain quadruples of spatial Fourier components, despite pairwise decorrelation. For the even/random isodipole texture pair, independent phase decorrelation greater than  $0.5\pi$  radians markedly reduced VEP indices of texture discrimination for all check sizes, and eliminated them entirely for check sizes of 8 min or greater. However, the product method preserved texture discrimination signals even with complete pairwise randomization of spatial phases. For the triangle/random isodipole texture pair, both kinds of phase decorrelation eliminated VEP indices of texture discrimination. These results imply that isodipole texture discrimination is based on fundamentally local processing, and not on global Fourier amplitudes—since the phase manipulations which eliminate texture discrimination preserve the Fourier amplitudes. The dependence of the antisymmetric response component (the odd harmonics) on phase decorrelation and texture type is consistent with a previously proposed model for feature extraction, and leads to constraints on how texture processing is modulated by contrast. The limited contribution of global spectral characteristics for small checks is consistent with a previously identified breakdown in scale-invariant processing. Copyright © 1996 Elsevier Science Ltd**

Textures   Evoked potentials   Spatial phase   Form perception

## INTRODUCTION

The importance of spatial frequency analysis in early visual processing is well-recognized (Campbell & Green, 1965; Kelly, 1972). For example, threshold behavior for a wide variety of visual patterns can be understood in terms of neural activity within a number of “channels”, each of which extract a range of spatial frequencies from the visual image (Wilson & Bergen, 1979). However, viewing the visual system as a parallel collection of independent channels, each of which is selective for a narrow range of spatial frequencies, does not suffice to account for suprathreshold phenomena. For example, one can readily perceive the difference between compound gratings (gratings consisting of superimposed sinusoidally varying luminance patterns) which differ in the spatial phases of the gratings (Nachmias & Weber, 1975; Burr, 1980; Badcock, 1984a,b). Additionally, spatial

phase sensitivity is one of the important differences between foveal and extrafoveal vision (Rentschler & Treutwein, 1985; Bennett & Banks, 1987).

Other evidence provides additional support for the importance of spatial phase in image recognition (Oppenheim & Lim, 1981; Field, 1987; Shapley *et al.*, 1990; Morgan *et al.*, 1991). While amplitude is important for overall image appearance (Tadmor & Tolhurst, 1992), phase information determines the placement of local features. Manipulation of images of real scenes which preserves power spectra but distorts the phase spectra destroys recognition; destruction of spectral information accompanied by retained spatial phase information preserves a recognizable image.

The above studies focused primarily on one-dimensional patterns or on natural scenes. In the studies described here, we investigate the extent to which the relative spatial phases of the individual Fourier components affect discrimination of visual textures. By restricting our attention to isodipole textures (Julesz *et al.*, 1978)—ensembles of two-dimensional stimuli which are balanced for spatial frequency content—we focus our investigation on the nonlinear processes underlying early

\*Department of Neurology and Neuroscience, Cornell University Medical College, 1300 York Avenue, New York NY 10021, U.S.A.

†To whom all correspondence should be addressed [Email jdvicto@med.cornell.edu].

visual processing. Because isodipole texture pairs have balanced second-order statistics, their discrimination cannot be due to differences in the overall power within any set of spatial frequency channels. Therefore, discrimination between isodipole textures must be due to: (i) higher-order statistics of individual Fourier components; or (ii) nonlinear local computations, or a combination of these possibilities. Since phase manipulations preserve the power spectrum, an observed dependence on relative spatial phase is inconsistent with mechanisms based on statistics of individual Fourier components (of any order). Conversely, specific models of local nonlinear mechanisms for feature extraction (Victor & Conte, 1991) predict specific patterns of dependence on spatial phase.

In view of the literature concerning the importance of relative spatial phase in other suprathreshold visual tasks, our finding that relative spatial phase plays a role in texture discrimination is not surprising. What is unexpected, however, is that one can manipulate spatial phases in a way which destroys all interrelations among the phases of pairs and triples of Fourier components, yet still retain strong discrimination. Such phase manipulations preserve visually apparent structure in one kind of isodipole texture [the “even” texture (Julesz *et al.*, 1978)], but not in another class [the “triangle” texture (Victor & Conte, 1991)]. As with studies of one-dimensional patterns (Badcock, 1984a,b; Morrone & Burr, 1988), there appears to be no need to postulate mechanisms which are specifically sensitive to spatial phase. Rather, these somewhat surprising results can be accounted for by a model for feature extraction that we have previously proposed (Victor & Conte, 1991). This model has as its key features two stages of nonlinearity: a small nonlinear subunit followed by a second stage at which the subunit outputs are combined in a cooperative fashion. The coupled dependence of response size on relative spatial phase and check size reveals additional information concerning the breakdown of scale—invariant processing at small check sizes. Furthermore, the difference between the dependence of response dynamics on stimulus contrast and on relative spatial phase provides new information concerning the cortical contrast gain control.

## METHODS

### Visual stimuli

The stimuli used in these studies are sequences of examples of isodipole textures—textures whose pairwise autocorrelations are identical (Julesz *et al.*, 1978). The stimuli are derived from the standard “even” (Julesz *et al.*, 1978), the “random”, and the “triangle” (Victor & Conte, 1991) isodipole textures via the following sequential stages:

- (i) Fourier transformation;
- (ii) low-pass filtering;
- (iii) partial or complete randomization of the phases of the Fourier components; and

- (iv) inverse Fourier transformation.

Examples of isodipole textures modified in this fashion are shown in Fig. 1.

### Isodipole textures

The standard isodipole textures consist of assignment of one of two states (luminance values) to a square array of checks: the luminance  $L$  at the position  $\mathbf{x}$  is given by  $L(\mathbf{x}) = L_0[1 + cf(\mathbf{x})]$ , where  $L_0$  is the background luminance,  $c$  is the contrast, and  $f(\mathbf{x})$  is  $+1$  or  $-1$ , depending on the state of the check containing  $\mathbf{x}$ . Check sizes ranged from 4 min ( $2 \times 2$  hardware pixels) to 32 min ( $16 \times 16$  hardware pixels). In the “random” texture, the state  $a_{i,j}$  assigned to the check in the  $i$ th row and  $j$ th column is chosen randomly, and with equal probability, from the two possibilities  $\pm 1$ .

In the “even” texture, the states  $a_{i,0}$  (the first column) and  $a_{0,j}$  (the first row) are chosen randomly. Checks in the interior of the texture are assigned states according to the recursion rule

$$a_{i,j} = a_{i-1,j} \cdot a_{i,j-1} \cdot a_{i-1,j-1}. \quad (1)$$

In the “triangle” texture, checks in the interior of the texture are assigned states according to the recursion rule

$$a_{i,j} = a_{i,j-1} \cdot a_{i-1,j-1}. \quad (2)$$

The fourth-order correlations induced by the recursion rule (1) and third-order correlations induced by the recursion rule (2) result in distinct patterns which are readily apparent to casual visual inspection, despite the absence of second-order correlations.

### Fourier transformation

To extract the Fourier components of the texture examples, we considered them to be periodic, with a period  $P$  equal to the extent of the display. This period was a multiple of the check size  $h$ , so that  $P = Nh$ , for some integer  $N$ . In these experiments,  $N = 16, 32, 64$ , and  $128$  for the four check sizes. The function  $f(\mathbf{x})$  which determines the contrast of the image at the position  $\mathbf{x}$  is therefore periodic, and its Fourier representation  $\hat{f}_{\text{unblurred}}(\mathbf{j})$  is given by

$$\hat{f}_{\text{unblurred}}(\mathbf{j}) = \frac{1}{P^2} \int_0^P f(\mathbf{x}) e^{-2\pi i \mathbf{j} \cdot \mathbf{x} / P} d\mathbf{x} \quad (3)$$

This integral ranges over two dimensions—in this case, a square of side length  $P$ . The (vector) argument  $\mathbf{j}$  is a pair of integers ( $j_1, j_2$ ) which enumerate the spatial frequencies that are consistent with the repeat  $P$ .

### Low-pass spatial filtering

Altering the phases of the Fourier components of the textures can lead to very high contrast values and oscillations at edges (“ringing”). For this reason, we applied spatial low-pass filtering of the textures prior to manipulation of the phases. The low-pass filter chosen had a roll-off at 4 c/deg, independent of check size. For the display size used ( $256 \times 256$  pixels subtending  $8.8 \times 8.8$  deg), this represented 32 cycles per screen,

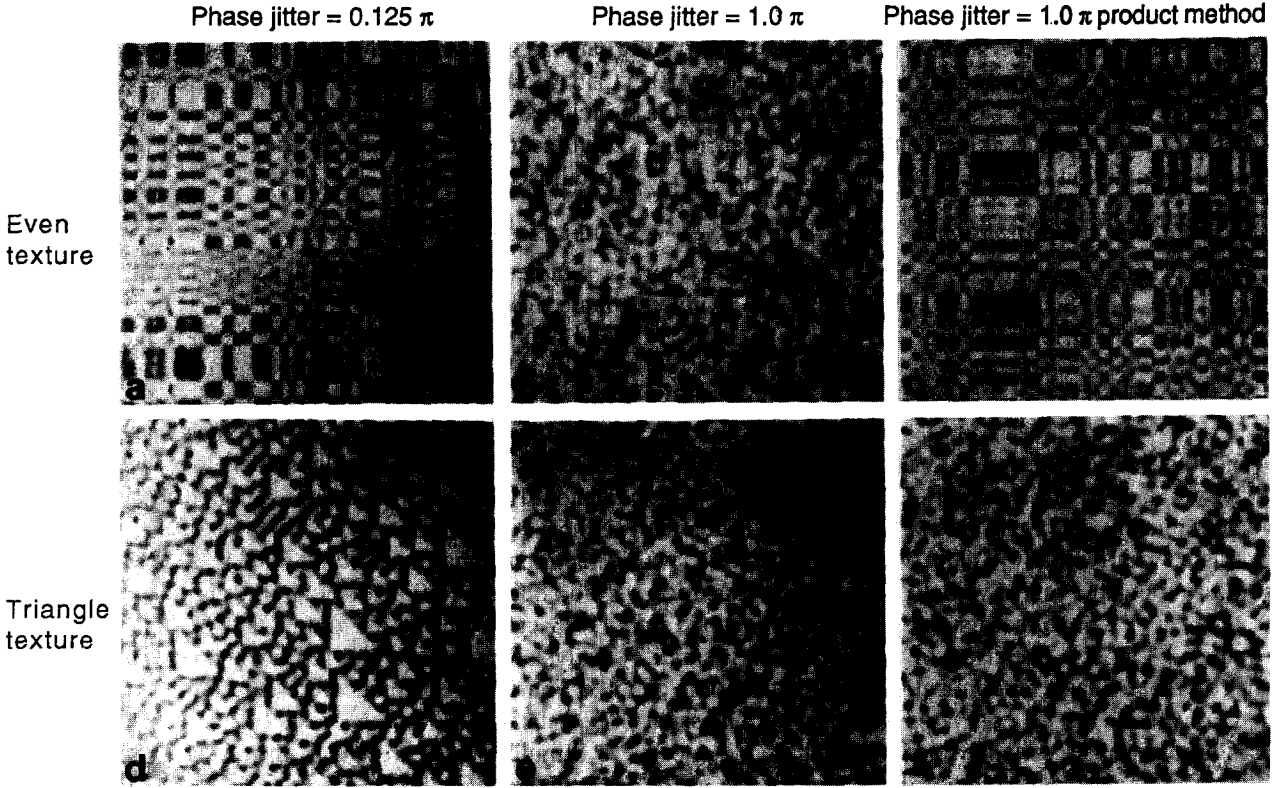


FIGURE 1. Examples of the stimuli used in this study. (a) An example of the even texture subjected to blurring followed by a small amount ( $\theta = 0.125\pi$ ) of phase decorrelation via the independent algorithm. (b) An example of the even texture subjected to blurring followed by maximal ( $\theta = \pi$ ) phase decorrelation via the independent algorithm. (c) An example of the even texture subjected to blurring followed by maximal phase decorrelation via the product method algorithm. (d), (e), and (f) examples of the triangle texture subjected to the phase manipulations of (a), (b), and (c).

and was 1/4 of the Nyquist frequency of the pixel display. That is, the Fourier components  $\hat{f}_{\text{blurred}}(\mathbf{j})$  of the low-pass filtered texture are given by

$$\hat{f}_{\text{blurred}}(\mathbf{j}) = e^{-|\mathbf{j}|^2 R_{\text{blur}}^2 / 4} \hat{f}_{\text{unblurred}}(\mathbf{j}), \quad (4)$$

where  $R_{\text{blur}} = 1/32$ .

The statistical properties referred to above are properties of the *ensemble* of textures of any given class: power spectra averaged over all examples of even textures created according to rule (1), or all examples of triangle textures created according to rule (2), are identical to power spectra averaged over all random textures. However, the power spectrum of *individual samples* of the even or triangle textures typically deviates from the power spectrum of *individual samples* of the random texture. One of the aims of this work is to determine to what extent these individual differences in the power spectrum play a role in texture discrimination. Low-pass filtering does not limit our ability to distinguish between the effects of phase manipulation and the effects of deviations of the power spectra of individual texture examples from that of the ensemble. Since the power spectrum depends on the amplitude (but not on the phase) of the spatial Fourier components, any effects of the phase manipulations described cannot be due to changes in the power spectrum, and the low-pass filtering affects

the power spectrum of structured and random textures identically.

#### Phase manipulation

Next, the phases of each Fourier component  $\hat{f}_{\text{blurred}}(\mathbf{j})$  are altered by an amount  $\beta(\mathbf{j})$  to provide the Fourier components of a phase-jittered texture sample  $\hat{f}_{\text{jittered}}(\mathbf{j})$ :

$$\hat{f}_{\text{jittered}}(\mathbf{j}) = e^{i\beta(\mathbf{j})} \hat{f}_{\text{blurred}}(\mathbf{j}) \quad (5)$$

We used two kinds of phase manipulation. In the first kind of phase jittering, which we call “independent” phase jittering, the phase shift  $\beta(\mathbf{j})$  associated with each Fourier component  $\hat{f}_{\text{blurred}}(\mathbf{j})$  was chosen uniformly from the distribution  $[-\theta, \theta]$ , subject only to the constraint

$$\beta(\mathbf{j}) = -\beta(-\mathbf{j}) \quad (6)$$

This constraint is required to ensure that the resulting Fourier coefficients correspond to a real image. The parameter  $\theta$  controls the amount of phase jitter:  $\theta = 0$  corresponds to no transformation of the image;  $\theta = \pi$  corresponds to complete phase randomization. Additionally, we used a “product method” to jitter the phases. In the product method, the phase shifts  $\beta(\mathbf{j})$  are required to conform to equation (6) and to

$$\beta(\mathbf{j}) = \beta_1(j_1) + \beta_2(j_2) \quad (7)$$

As in the “independent” phase-jittering method, the phase shifts at two distinct frequencies  $\mathbf{j}$  and  $\mathbf{k}$  (with

$j \neq \pm k$ ) are independent. However, in the product method, the phase factor  $e^{i\beta(j)}$  at the spatial frequency  $j = (j_1, j_2)$  is given by the product of the phase factors at the spatial frequency  $(j_1, 0)$  and the spatial frequency  $(0, j_2)$ . These phases are chosen randomly from the distribution  $[-\theta, \theta]$ , subject only to the real-image constraint [equation (6)].

### Inverse Fourier transformation

The final image is defined by  $L_{\text{jittered}}(\mathbf{x}) = L_0[1 + cf_{\text{jittered}}(\mathbf{x})]$ , where  $f_{\text{jittered}}(\mathbf{x})$  is given by the inverse Fourier transform

$$f_{\text{jittered}}(\mathbf{x}) = \sum_j \hat{f}_{\text{jittered}}(j) e^{2\pi i j \cdot \mathbf{x} / P} \quad (8)$$

The distribution of image values  $f_{\text{jittered}}(\mathbf{x})$  spans a wider range than the range  $[-1, +1]$  covered by the image values  $f_{\text{blurred}}(\mathbf{x})$  in the starting texture. Since the contrast  $c$  was typically 0.4 for the starting texture, we therefore truncated image values of the inverse transform  $f_{\text{jittered}}(\mathbf{x})$  at  $\pm 2.5$ , so that its pixel contrasts remained in the range  $[-1, +1]$ . The effect of this truncation is small. For complete phase randomization, the distribution of image values in  $f_{\text{jittered}}(\mathbf{x})$  approaches a Gaussian distribution whose variance matches that of  $f_{\text{blurred}}(\mathbf{x})$ , and therefore exceeds 2.5 in absolute value  $<1.4\%$  of the time. In one set of studies (see Fig. 5), higher contrast stimuli were used, which necessarily results in greater truncation for values of  $\theta > 0$ . However, the critical comparison in that experiment is that of the stimuli for which  $c = 0.4$  and  $\theta > 0$  with stimuli for which  $c > 0.4$  and  $\theta = 0$ . Truncation is negligible in both of these regimes.

### Incorporation of modified isodipole textures into visual stimuli

The visual stimuli for these experiments consisted of presentations of precomputed images  $L_{\text{jittered}}(\mathbf{x})$ , which alternated between examples of a structured texture (the even texture or the triangle texture) and a random texture. The stimulus sequence is organized around a period of 473 msec (128 frames of the hardware display). A structured texture is presented at the beginning of each period, and a random texture is presented in the middle of each period (64 frames, or 236.5 msec later). Successive presentations of each texture type consisted either of the same texture pair inverted in contrast, or of new examples of the texture.

Within each recording session, the main experimental variable was the amount  $\theta$  of phase jitter. The stimuli used within each recording session were always constructed from the *same examples* of unjittered textures. That is, the Fourier amplitudes of these stimuli were *exactly* matched across amounts of phase jitter.

### Production of visual stimuli

Precomputed visual stimuli described above were produced on a Tektronix 608 display which subtended  $8.8 \times 8.8$  deg at a viewing distance of 57 cm and had a mean luminance of 150 cd/m<sup>2</sup>. Control signals for the stimulator were produced by specialized electronics,

modified from the design of Milkman *et al.* (1980) interfaced to a DEC 11/73 computer. These electronics generated horizontal and vertical scan signals for a  $256 \times 256$  pixel display at a frame rate of 270.3 Hz, and included a digital look-up table which corrected for the nonlinear intensity/voltage relationship of the display oscilloscope.

### Subjects and VEP recording

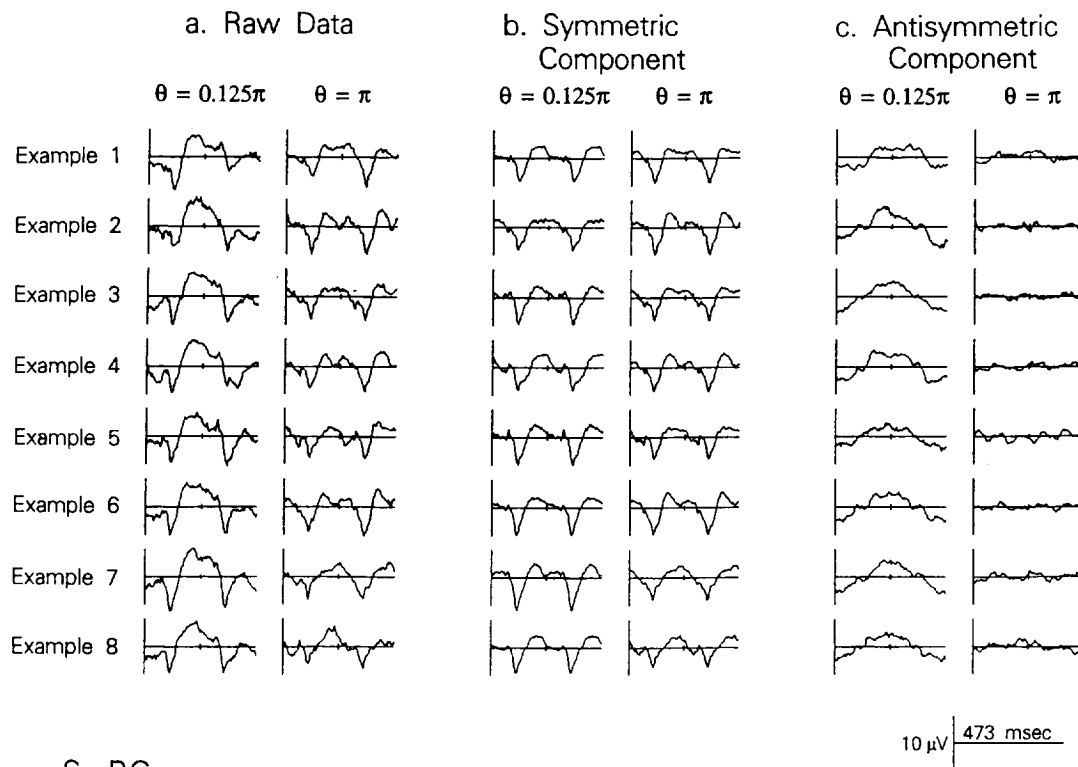
Studies were conducted on six normal subjects (two male, four female) who ranged in age from 25 to 43 yr, and had visual acuities (with correction if necessary) of 20/20 or better. One subject (KE) participated only in the first experiment. Subjects were instructed to fixate binocularly on a fixation point placed at the center of the visual stimulus. Scalp signals were obtained from standard gold cup electrodes, applied to the scalp with Nihon-Kohden electrolyte paste at C<sub>z</sub> (+) and O<sub>z</sub> (-). Electroencephalographic activity was amplified 10,000-fold, filtered (0.03–100 Hz) and digitized by the DEC 11/73 computer at the frame rate of 270.3 Hz. Fourier analysis was carried out on-line, and confidence limits of the Fourier coefficients were determined off-line by the  $T_{\text{circ}}$  statistic (Victor & Mast, 1991).

Stimuli were presented in 65 sec runs of texture alternation. The initial portion of each run was discarded. The remaining 60.5 sec of the recording, which comprised responses to 128 presentations of each kind of texture, was averaged with respect to the stimulus period of 473 msec. Recording sessions were organized in groups of 64–128 runs, consisting of four to eight examples of each run type. Within sessions, the order of the different run types was randomized in blocks.

## RESULTS

### Initial observations: sensitivity to spatial phase

In the first experiment, we examined responses to alternations of even and random textures subjected to either a small amount of phase jitter ( $\theta = 0.125\pi$ : spatial phases jittered by up to 1/8 of a cycle) or complete randomization of spatial phases ( $\theta = \pi$ ). Textures had a contrast of 0.4 prior to phase jittering, and the check size was 8 min. In this initial experiment, we were concerned about the possible dependence of responses on the selection of individual examples of the even and the random textures. Therefore, the experiment was organized as eight kinds of runs for each condition ( $\theta = 0.125\pi$  or  $\theta = \pi$ ), each with a different *single* example of textures and a different choice of random values for phase jitter within the allowed range. The even and random texture examples used to generate the stimuli for the low phase jitter condition ( $\theta = 0.125\pi$ ) and the high phase jitter condition ( $\theta = \pi$ ) were the same; these stimuli differed only by the amount of phase jitter. Each of the 16 conditions (eight pairs of texture examples and two levels of phase jitter) was presented for four 1 min runs, so that effects of texture example, phase jitter, and random run-to-run variability could be distinguished.



S: BG

FIGURE 2. Responses elicited by alternation between examples of even and random textures subjected to small amounts ( $\theta = 0.125\pi$ ) and large amounts ( $\theta = \pi$ ) of phase jitter. In each panel, the two responses in each row correspond to stimuli based on the same examples of even and random textures, which differ only in the amount of phase jitter. Responses within a single column correspond to stimuli based on different examples of even and random textures, but the same amount of phase jitter. (a) Raw averages. (b) Symmetric response component. (c) Antisymmetric response component. Check size: 8 min. Contrast (prior to phase jittering): 0.4. Subject: BG.

Visual evoked potentials (VEPs) obtained from one subject are shown in Fig. 2. In both cases, the responses to the different texture examples which share the same amount of phase jitter are nearly identical. On the other hand, there are dramatic differences in the responses to textures which have the same spatial frequency content but a different amount of phase jitter. This is most clearly seen by decomposing responses into a symmetric response component, consisting of the even harmonics, and an antisymmetric component, consisting of the odd harmonics (Victor, 1985; Victor & Zemon, 1985; Victor & Conte, 1987, 1991). The even harmonics contain the average of the responses to the two kinds of textures; the odd harmonics contain the difference between the responses to the two kinds of textures.

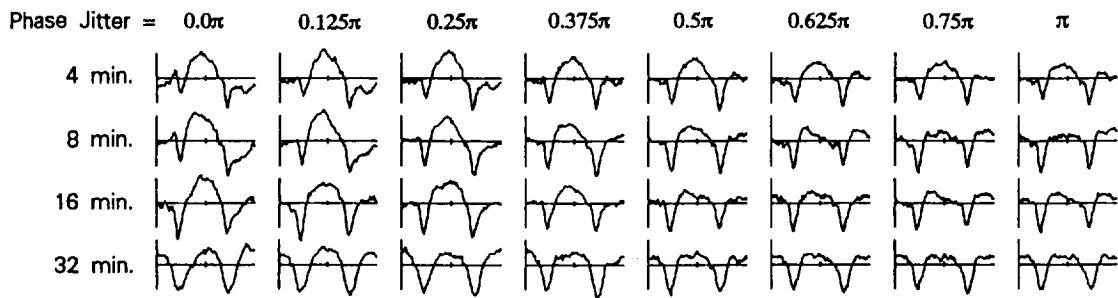
As seen in Fig. 2, the symmetric response component to textures with either a small amount of phase jitter ( $\theta = 0.125\pi$ ) or a maximal phase jitter ( $\theta = \pi$ ) are similar, consisting of a brief occiput-positive component with a latency of 100–120 msec following each texture interchange. However, the antisymmetric response component was prominent only for the condition with a small amount of phase jitter, and had much slower dynamics. The responses to the textures with a small amount of phase jitter are similar to responses elicited by interchange between structured and random textures with sharp edges and no phase jitter, and the responses to the

textures with a large amount of phase jitter are similar to those elicited by interchange between different examples of random textures (Victor & Conte, 1989, 1991).

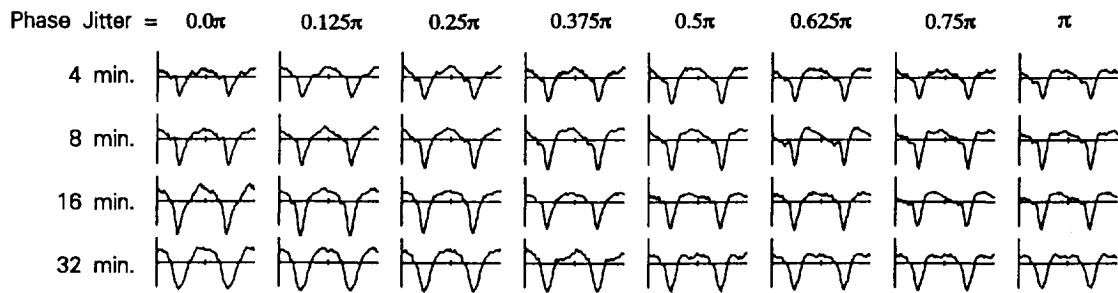
For this subject, the antisymmetric response, as quantified by the amplitude of the first harmonic, averaged across all texture examples, was 2.32  $\mu\text{V}$  in the low phase jitter ( $\theta = 0.125\pi$ ) condition, but was reduced to 0.14  $\mu\text{V}$  in the maximal phase jitter ( $\theta = \pi$ ) condition. The symmetric response, as quantified by the amplitude of the second harmonic, was similar in these two conditions: 2.00 for  $\theta = 0.125\pi$ , and 1.87 for  $\theta = \pi$ . Across all subjects, increasing phase jitter reduced the first-harmonic response amplitude by 62–98% (average of 87%), while second harmonics were reduced slightly in four subjects and augmented in two subjects (23% reduction to 21% augmentation, average of 2% reduction).

The marked dependence of the first harmonic on phase jitter is in contrast with its independence of the choice of texture example. For the subject shown in Fig. 2, the dependence of the amplitude of the first harmonic on choice of texture example amounted to 21% of the response amplitude (4% of the power) in the low phase jitter condition; for the six subjects, the average dependence of the amplitude on texture example was 26%. Second-harmonic responses showed a similarly

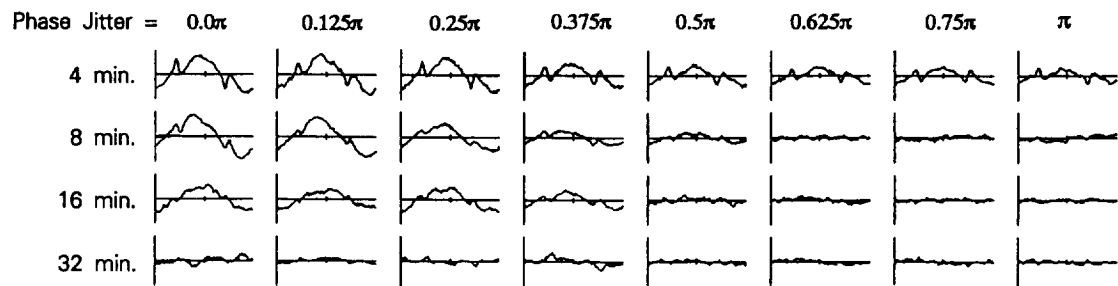
## a. Raw Data



## b. Symmetric Component



## c. Antisymmetric Component



10  $\mu$ V | 473 msec

S: JV

FIGURE 3. Responses elicited by alternation between examples of even and random textures subjected to graded amounts of phase jitter, for four check sizes. (a) Raw averages. (b) Symmetric response component. (c) Antisymmetric response component. Contrast (prior to phase jittering): 0.4. Subject: JV.

small dependence on texture example: 21% for  $\theta = 0.125\pi$  and 22% for  $\theta = \pi$ .

To determine whether the dependence on texture example was more than that due to chance alone, we compared the response variability across choices of texture example to the response variability within replicate runs of the same texture example. For this comparison, we used an analysis of variance based on the  $T_{\text{circ}}$  statistic (Victor & Mast, 1991), a statistic which is specifically suited to the detection of steady-state evoked potentials and appears near-optimal (Dobie & Wilson, 1993) in this regard. Two subjects (JV and MC) showed a "significant" dependence ( $P < 0.05$ ) of the first harmonic on texture example for both levels of phase jitter, and a third subject (SM) showed a significant dependence only in the maximal phase-jitter condition ( $\theta = \pi$ ). Two subjects (JV and RB) showed a significant dependence of the second harmonic on texture example for  $\theta = 0.125$ ,

and one (KE) showed a significant dependence on second harmonic for  $\theta = \pi$ .

In sum, our major finding was that the antisymmetric response component elicited by isodipole texture interchange was essentially abolished by a full randomization of phase ( $\theta = \pi$ ). Secondarily, this change could not be accounted for by the choice of the texture example. The dependence on texture example was small (c. 20% of amplitude, or 4% of variance), but did reach statistical significance in some subjects. Therefore, in the later experiments, in which we explored dependence on amount of phase randomization, check size, or contrast, we averaged over runs in which at least four different examples of the textures were used.

#### Interaction of phase manipulation and check size for the even textures

In the next experiment, we examined the dependence

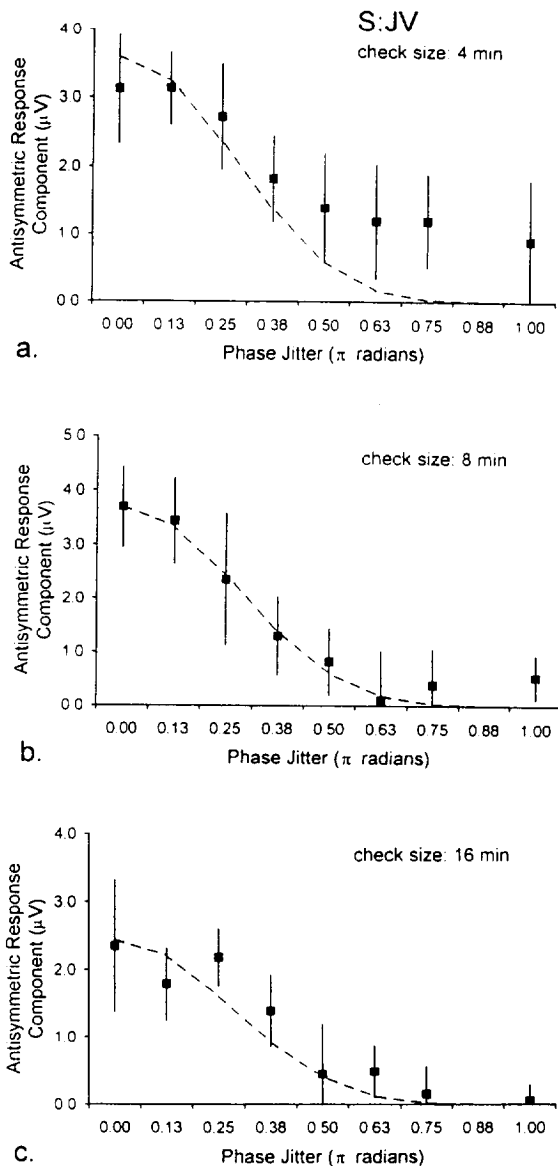


FIGURE 4. Size of antisymmetric response, as measured by the first harmonic amplitude, elicited by alternation between examples of even and random textures subjected to graded amounts of phase jitter. The dashed lines are a fit of the data to  $K[(\sin \theta)/\theta]^4$ . Error bars are 95% confidence limits as determined by  $T_{\text{circ}}$ . (a) 4 min checks; (b) 8 min checks; (c) 16 min checks. Data of Fig. 3.

of the symmetric and antisymmetric response components on the degree of phase jitter and on check size. We used independent jittering of phases, ranging from no phase jitter ( $\theta = 0$ ) to maximal phase jitter ( $\theta = \pi$ ) in steps of  $0.125\pi$ , and check sizes ranging from 4 to 32 min.

Data obtained from one subject are shown in Fig. 3. As seen in (a), responses generally contain a mixture of symmetric and antisymmetric components. The symmetric component, shown in (b), is nearly independent of phase jitter, and steadily increases in amplitude with increasing check size. The antisymmetric component, shown in (c), depends strongly on the amount of phase jitter. For textures with no phase jitter (i.e. subjected only to low-pass spatial filtering), the antisymmetric response is largest for 8 and 16 min checks, and is not significantly

different from zero for 32 min checks (via  $T_{\text{circ}}$  with 95% confidence limits). These findings are consistent with the spatial tuning previously reported for VEPs elicited by unblurred isodipole textures (Victor & Zemon, 1985). However, for complete randomization of phases ( $\theta = \pi$ ), the antisymmetric response is only significantly different from zero for the 4 min checks.

The dependence of the size of the antisymmetric response, as measured by the amplitude of the first Fourier component, is analyzed in more detail in Fig. 4. For 8 and 16 min checks, response size drops essentially to zero for  $\theta = 0.5\pi$ . For 4 min checks, the response size drops rapidly over the range from  $\theta = 0$  to  $\theta = 0.5\pi$ , and then remains constant for larger amounts of phase jitter. This corresponds well with informal psychophysical observations: for the larger check sizes, the phase-jittered even textures become indistinguishable from phase-jittered random textures for  $\theta = 0.375\pi - 0.5\pi$ ; for 4 min check sizes, the even textures remain minimally distinguishable over the entire range of phase-jittering. The dashed lines in Fig. 4 correspond to the function  $K[(\sin \theta)/\theta]^4$ . This is the functional form expected for the size of the antisymmetric response (see below) in the limit of purely local processing, and is seen to be a good fit for the 8 and 16 min checks, but not 4 min checks.

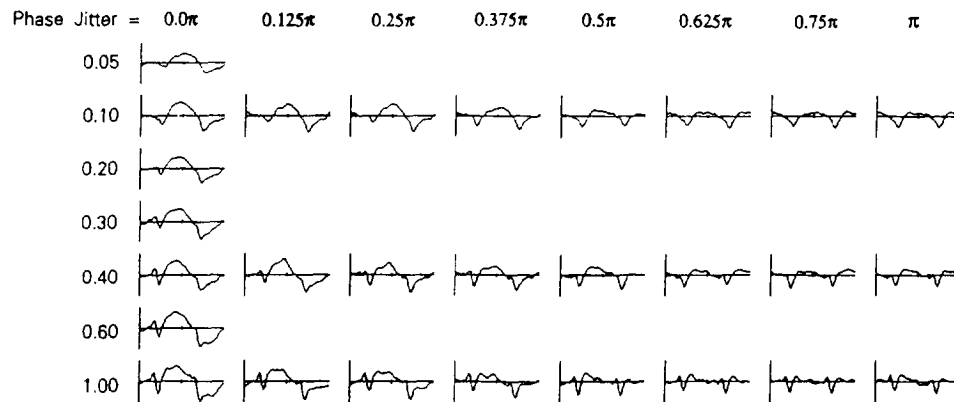
These VEP findings held across the other four subjects. In all subjects, there was a significant antisymmetric response to 4 and 8 min checks for  $\theta = 0$ , and for four of the five subjects, there was a significant antisymmetric response to 16 min checks for  $\theta = 0$ . For 4 min checks, the response remained significant at  $\theta = \pi$  in four of the five subjects, but had an amplitude which averaged 38% of the amplitude of the response to theunjittered textures. However, for 8 and 16 min checks, complete phase jittering resulted in responses which were not significantly different from 0 for any of the subjects. No subject had significant antisymmetric responses to the textures created from 32 min checks.

#### Dependence on contrast

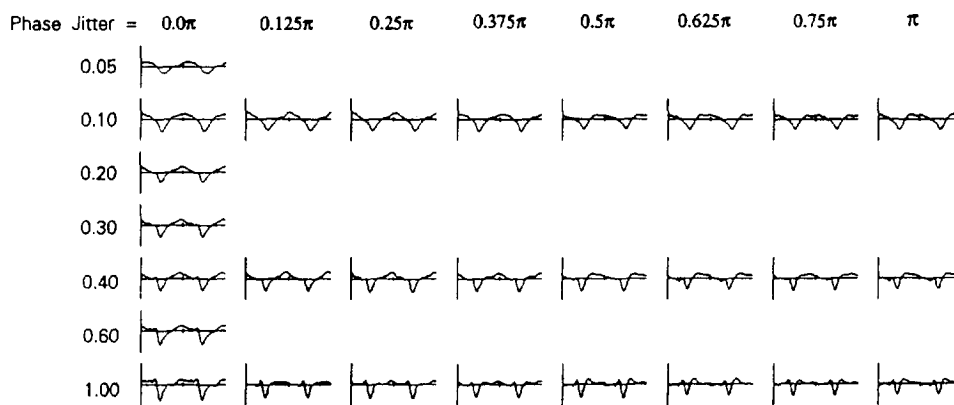
The next experiment compared the effects of phase jitter with the effects of overall changes in contrast. As seen in Fig. 5, the attenuation of responses due to increased phase jitter is not comparable to the attenuation of responses due to decreased contrast. Increasing amounts of phase jitter leave the symmetric response component [Fig. 5(b)] unchanged, while the antisymmetric response component [Fig. 5(c)] is reduced essentially to zero at  $\theta = 0.5\pi$ . Contrast changes over the range 0.05–1.0 have only modest effects on the amplitude of both symmetric and antisymmetric components. However, response phase is affected by overall contrast and not by phase jitter. Responses at higher contrasts show a relative phase lead in comparison to low contrast responses, but there is no change in temporal response phase (of either symmetric or antisymmetric response components) as phase jitter increases from  $\theta = 0$  to  $\theta = \pi$ . This is illustrated for the antisymmetric component in Fig. 6.

S: JV

## a. Raw Data



## b. Symmetric Component



## c. Antisymmetric Component

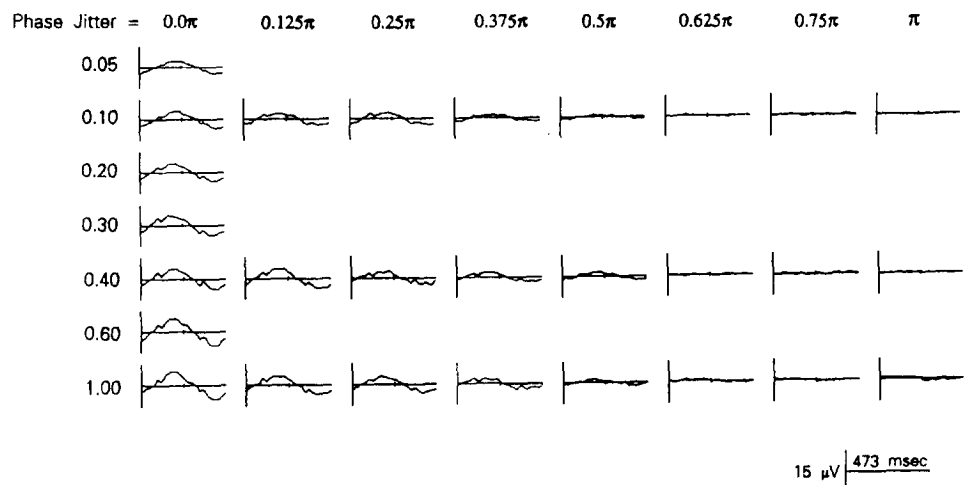


FIGURE 5. Comparison of the effects of graded amounts of phase jitter and contrast. (a) Raw averages. (b) Symmetric response component. (c) Antisymmetric response component. Check size: 8 min. Subject: JV.

Other subjects showed similar trends. For blurred textures without phase jitter, response amplitude depended only weakly on contrast, increasing typically by a factor of 2 over the range 0.05–1.0 (range: 1.02–2.46, geometric mean: 1.70). In all subjects, response phases showed increasing phase lead with increasing contrast (range:  $0.04$ – $0.42\pi$  radians, mean  $0.24\pi$  radians), but

there was no consistent dependence of response phase on the amount of phase jitter.

*The effects of product–method manipulation of phase on the even textures*

In the previous experiments, we used a phase randomization algorithm (the independent method)



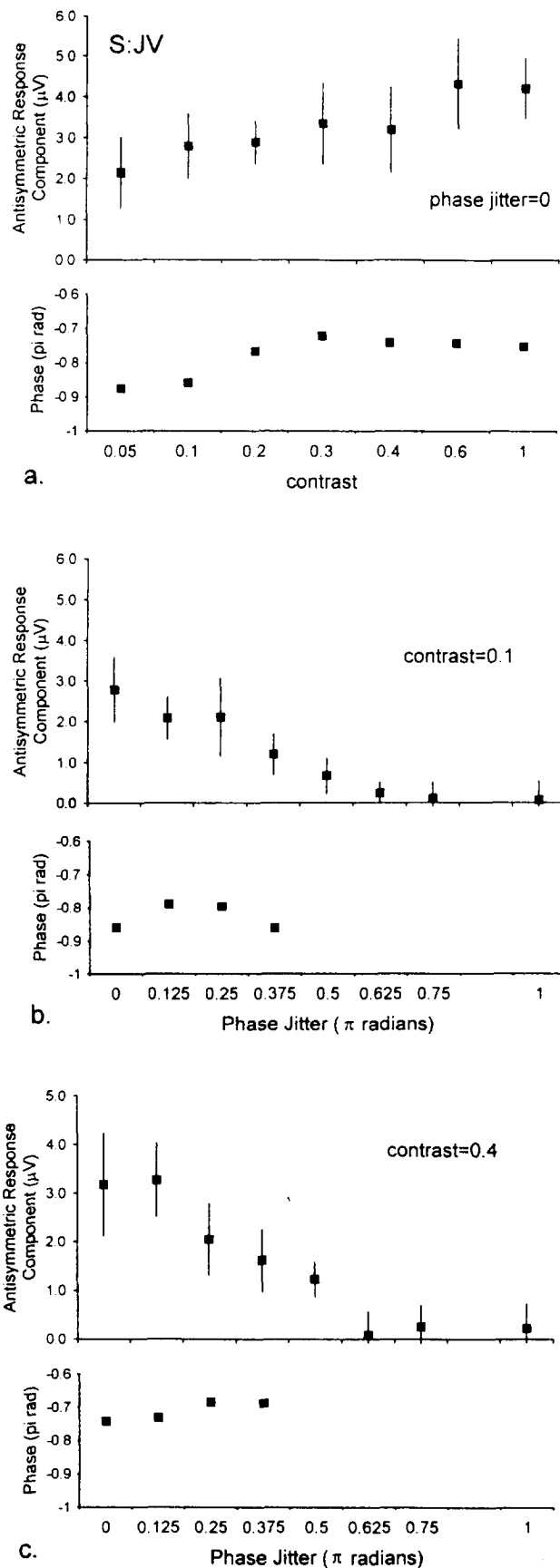


FIGURE 6. Size of antisymmetric response, as measured by the first harmonic amplitude, and phase of first harmonic response elicited by alternation between examples of blurred even and random textures over a range of contrasts (a) and as a function of phase jitter for contrasts of 0.1 (b) and 0.4 (c). Error bars are 95% confidence limits as determined by  $T_{\text{circ}}$ . Phase data are only shown for responses which are significantly different from zero. Data of Fig. 5.

which destroyed correlations of all orders among the Fourier components. In the next set of experiments, we used a phase randomization algorithm (the product method, as described in Methods) which eliminated phase correlations between pairs and triples of Fourier components, but preserved correlations among certain quadruples of Fourier components. The comparison of the VEPs elicited by textures with these two kinds of phase decorrelation used stimuli based on precisely the same examples of the even and random textures.

Typical results are shown in Fig. 7. As described above, textures subjected to independent phase jittering provided little antisymmetric response for phase jitters of  $\theta = 0.5\pi$  or greater. However, textures subjected to phase jittering by the product method, which preserves certain higher-order phase correlations, elicited significant antisymmetric response components for all values of the phase jitter. Indeed, there was no detectable dependence of the amplitude or phase of the first-harmonic response on the amount of phase jitter, provided that phase jitter was introduced by the product method.

Across the four subjects studied, the ratio of the amplitude of the first harmonic response for maximal independent phase jitter to the response without phase jitter ranged from 0.07 to 0.26 (geometric mean 0.13)—i.e. it was essentially eliminated with maximal phase jitter. However, with phase jitter by the product method, the ratio of the first harmonic response with maximal jitter to the response without phase jitter ranged from 0.79 to 1.35 (geometric mean 1.02). Thus, the correlations in phase that are preserved by the product method suffice to preserve the antisymmetric response component, despite the loss of all pairwise and three-frequency phase correlations.

#### *The effects of phase manipulation on the triangle textures*

In the final set of experiments, we investigated whether the effect of phase manipulation on responses to alternation between the even and random textures generalized to other isodipole texture interchanges. In these experiments, the triangle texture [defined by equation (2)] was substituted for the even texture. We chose the triangle texture because: (i) it is a third-order texture, as opposed to the even texture, which is fourth-order; and (ii) VEPs elicited by interchange between the triangle texture and the random texture had dynamics which differed from those elicited by even/random interchange, which suggested that these two textures may drive different mechanisms (Victor & Conte, 1991).

As in the previous experiments, we used a stimulus period of 473 msec, in which the first half contained a triangle texture, and the second half contained a random texture. In alternate periods, the contrast of the stimulus was inverted. For the even texture, this contrast-inversion merely generated new examples of the even texture, and provided a means for balancing local luminance across the texture examples. For the triangle texture, contrast inversion also provides luminance balance, but at the expense of converting textures which have prominent

## S: RB

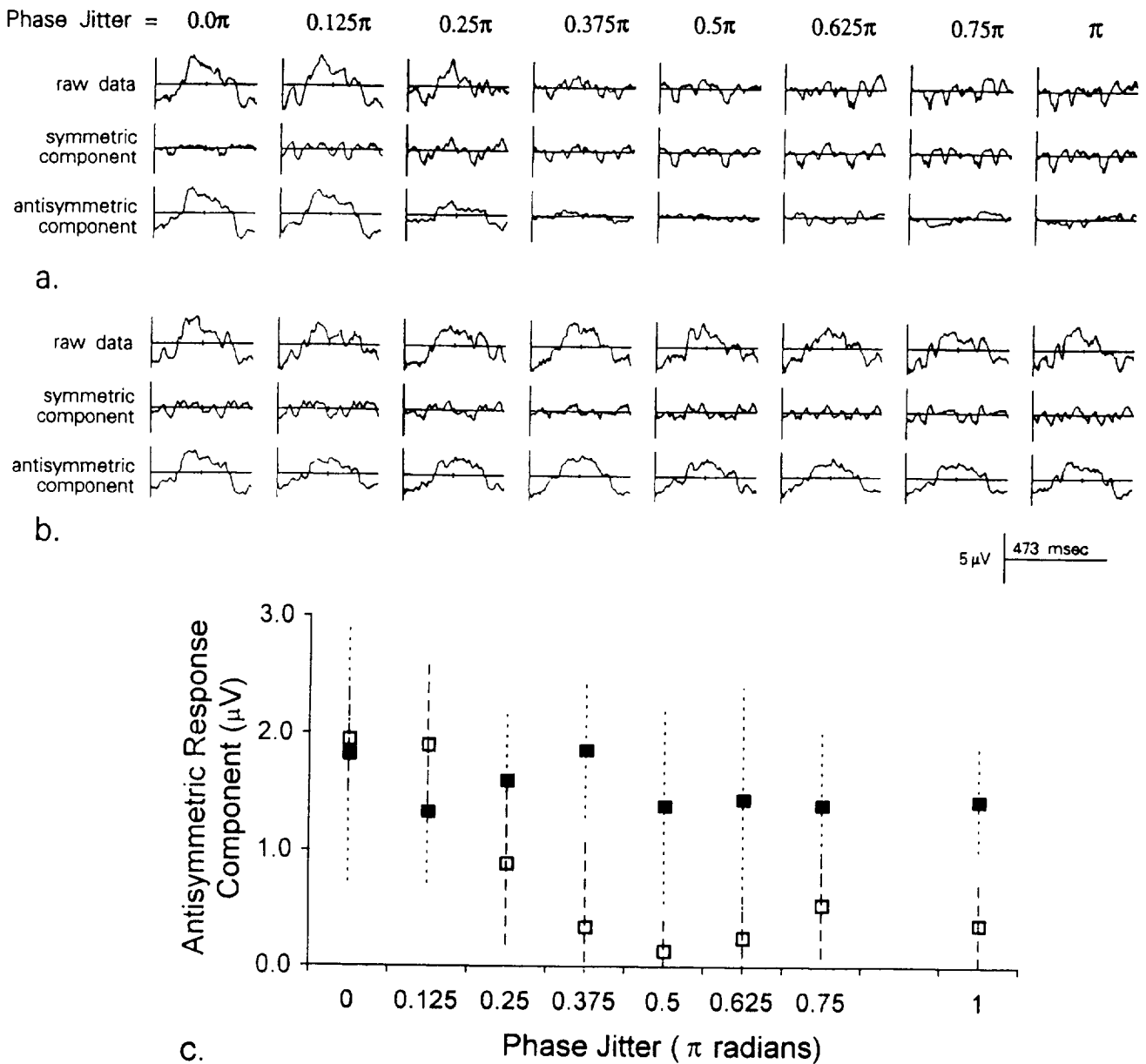


FIGURE 7. Comparison of the effects of independent and product method phase jitter for the even texture. (a) Raw, symmetric, and antisymmetric components as a function of independent phase jitter. (b) Raw, symmetric, and antisymmetric components as a function of phase jitter via the product method. The product method induces random, uncorrelated shifts between pairs of Fourier components, but preserves certain phase relationships between quadruples of Fourier components. The responses of (a) and (b) were recorded on separate days. (c) Size of antisymmetric response, as measured by the first harmonic amplitude, of the responses shown in (a) and (b). Open symbols: independent method; solid symbols: product method. Error bars are 95% confidence limits as determined by  $T_{\text{circ}}$ . Check size: 8 min. Contrast (prior to phase jittering): 0.4. Subject: RB.

bright triangles into textures which have prominent dark triangles. Previously (Victor & Conte, 1991), we showed that VEP responses to these two different polarities of triangle textures are identical, a result which we confirmed in this study by comparing responses to alternate stimulus periods. Responses from these alternate stimuli periods were therefore averaged together.

The effect of phase jitter on the VEPs elicited by alternation between the triangle texture and the random texture are shown in Fig. 8. As in the case of the even

textures, triangle textures subjected to independent phase jittering provided no significant antisymmetric response for phase jitters of  $\theta = 0.375\pi$  or greater (a and c). The symmetric response, as assayed by the second harmonic, was essentially independent of phase jitter (a and d). The same behavior was seen for phase jittering by the product method (b, c, and d): the antisymmetric response disappeared for phase jitters of  $\theta = 0.375\pi$  or greater (b and c), while the symmetric response was independent of phase jitter (b and d).

S: MC

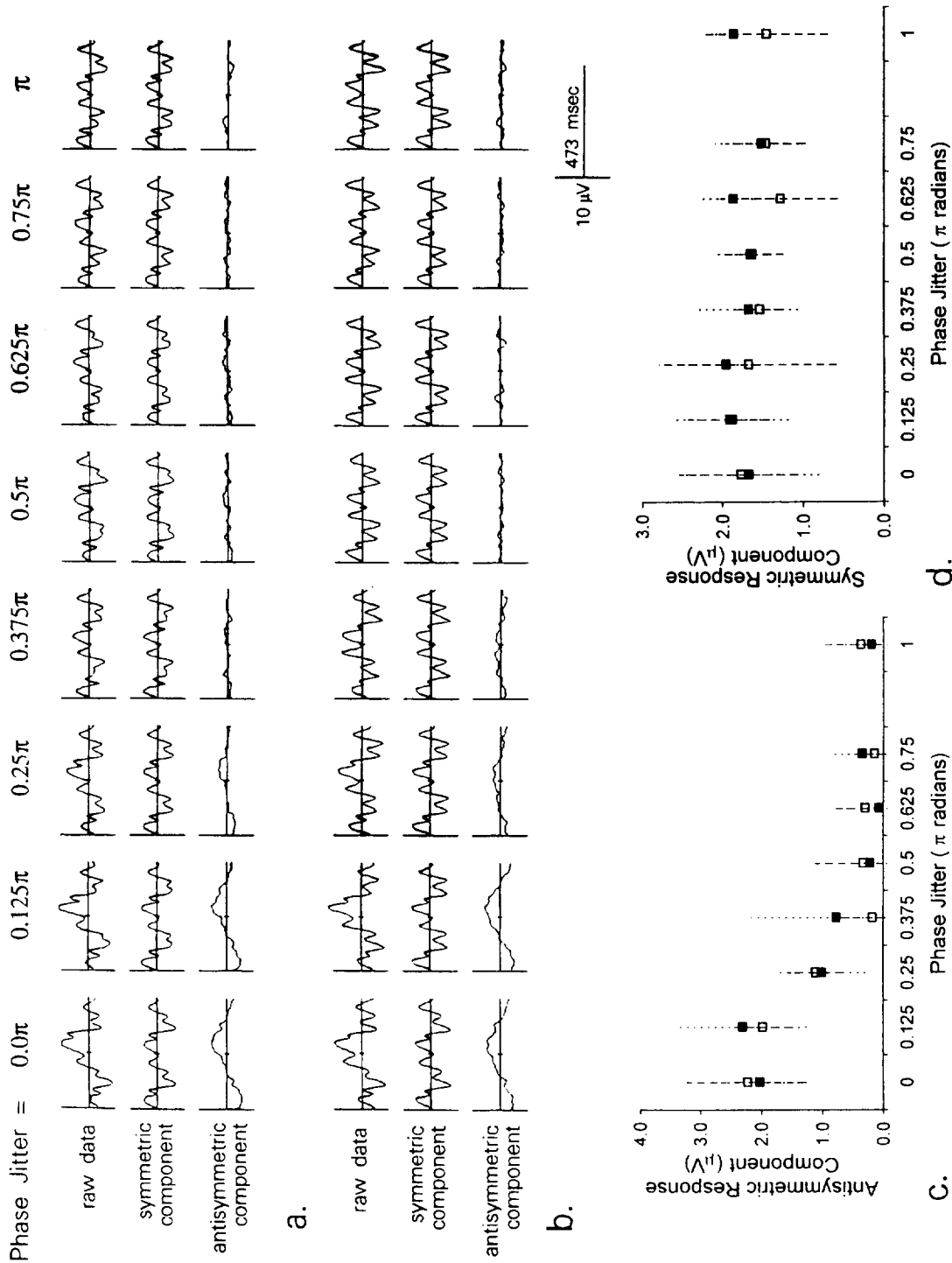


FIGURE 8. Comparison of the effects of independent and product method phase jitter for the triangle texture. (a) Raw, symmetric, and antisymmetric components as a function of independent phase jitter. (b) Raw, symmetric, and antisymmetric components as a function of phase jitter via the product method. (c) Size of antisymmetric response, as measured by the first harmonic amplitude, of the responses shown in (a) and (b). (d) Size of symmetric response, as measured by the second harmonic amplitude, of the responses shown in (a) and (b). Error bars are 95% confidence limits as determined by  $T_{\text{circ}}$ . Check size: 8 min. Contrast (prior to phase jittering): 0.4. Subject: MC.

This experiment was performed in two other subjects (JV and RB), with similar results. The symmetric response was relatively independent of either kind of phase jitter (no significant change in any of the subjects). However, the antisymmetric response was sharply attenuated by either kind of phase jitter. In all subjects, the first harmonic response was not significantly zero at  $\theta = 0.5\pi$  or greater. With independent phase jitter of  $\theta = 0.375\pi$ , the first harmonic averaged 24% of its size in the absence of phase jitter. With product method phase jitter, the first harmonic averaged 35% of its size in the absence of phase jitter. This is in marked contrast to the interaction of phase jitter with the responses to the even/random interchange. For the even/random texture, independent phase jitter attenuates the response, but product-method phase jitter does not (Fig. 7); for the triangle texture, both kinds of phase jitter attenuate the response.

One can readily understand the loss of VEP amplitude seen with product-method decorrelation of the triangle texture: the product method primarily retains correlations along the horizontal and vertical axes, and these axes are not very important for this texture. This emphasizes that the antisymmetric VEP response is not driven by the global phase statistics *per se*, but rather on particular spatial features of the stimuli.

## DISCUSSION

### *Summary of results*

We studied the role of spatial phase in the analysis of visual form. In order to focus on processes beyond simple spatial filtering, we studied VEP responses to interchange of isodipole textures. The odd harmonics of this response ("the antisymmetric response component") contain the difference of the responses to two textures. The statistical properties of the textures (in the ensemble sense) eliminate responses driven by local luminance, contrast, or spatial frequency differences, and the size of the antisymmetric response component correlates well with psychophysical discriminability (Victor & Conte, 1987, 1989, 1991). In this study, we have quantified the antisymmetric response size by the amplitude and phase of the first harmonic, and use this as an index of discriminability. Conversely, the even harmonics ("the symmetric response component") resemble the traditional P-100 and contain contributions from mechanisms sensitive to contrast changes, independent of texture identity (Victor, 1985; Victor & Zemon, 1985; Victor & Conte, 1989, 1991). We have therefore used the amplitude and phase of the second harmonic as an index of response to contrast changes, independent of spatial pattern.

Our main findings are:

- (i) The size of the antisymmetric VEP response is markedly attenuated when the phases of the spatial Fourier components are jittered. For "even" textures based on pixels of 8 and 16 min, the antisymmetric response is essentially zero when phases are subjected to randomization by  $0.5\pi$  radians or more. For textures based on pixels of 4 min, the antisymmetric response is attenuated by phase jitter, but remains nonzero even for full phase randomization.
- (ii) The reduction in antisymmetric response size with increasing phase jitter was not accompanied by a change in phase of the antisymmetric response component, nor a change in the amplitude or phase of the symmetric response component. This is in distinction to the effect of decreasing contrast, which attenuates the size of antisymmetric and symmetric response components, and produces a relative phase lag.
- (iii) Randomization of phases by a method which destroys all pairwise and third-order phase relationships but preserves certain fourth-order phase relationships ["the product method" of equation (7)] results in preservation of the antisymmetric response to even/random interchange, for all amounts of phase jitter.
- (iv) For interchange between the triangle and the random texture, the antisymmetric response disappears for phase jitters of  $0.375\pi$  or greater, whether the phases are independently jittered or subject to the constraint of equation (7).

### *Texture discrimination: Local vs global*

Multiple lines of evidence indicate that texture discrimination requires nonlinear processing of the visual input. Within the broad class of nonlinear models, one may identify two extremes along a continuum: models in which local nonlinearities are prominent, and models based primarily on global nonlinearities (i.e. linear filtering followed by a decision process). The local vs global distinction, though very useful conceptually, is surprisingly difficult to formalize, because a global nonlinear process can typically be recast as a sum of local nonlinearities. Additive pooling of receptive field outputs followed by a single nonlinearity is computationally equivalent to a model which sums the outputs of nonlinearities operating on each receptive field output, along with a series of contributions from interactions among receptive fields. Because of this fundamental ambiguity, we have resorted to a somewhat more abstract approach to formalizing this conceptual distinction.

Any computational model presented in terms of receptive field profiles, dynamical elements, and nonlinearities—the spatial domain—can be recast into the Fourier domain. This is because the Fourier transform of the visual image (an assignment of amplitude and phase to each spatial frequency) preserves all of the information in the image, and thus, any calculation performed on the image can be performed on its transform. A nonlinearity in the spatial domain will thus translate into a multiplicative interaction between two or more components of the Fourier representation.

The Fourier transform of a visual image  $f(\mathbf{x})$  consists of

a set of complex-valued quantities  $\tilde{w}(\mathbf{k})$ , one at each spatial frequency  $\mathbf{k}$ , and we think of each Fourier component  $\tilde{w}(\mathbf{k})$  in terms of its amplitude and phase. Translation of the visual image (a spatial shift of a visual image  $f(\mathbf{x})$  by an amount  $\Delta\mathbf{x}$ ) corresponds to multiplication of the Fourier transform  $\tilde{w}(\mathbf{k})$  at the spatial frequency  $\mathbf{k}$  by  $e^{i\mathbf{k}\cdot\Delta\mathbf{x}}$ . This multiplicative factor necessarily leaves the amplitude unchanged, but can shift the phase to arbitrary values. Thus, while Fourier amplitudes can be used for texture discrimination or object identification, the *absolute* spatial phase of an *individual* Fourier component cannot—even though spatial phase is known (Oppenheim & Lim, 1981; Field, 1987; Shapley *et al.*, 1990; Morgan *et al.*, 1991) to be critical for object identification. Thus, Fourier analysis identifies two sources of information for texture discrimination or object identification: the amplitude of individual Fourier components, and the *relative* spatial phases of two or more Fourier components.

Any spatial nonlinearity has the potential to generate relative spatial phase information, since multiplicative interactions in the spatial domain will translate into multiplicative interactions among two or more Fourier components  $\tilde{w}(\mathbf{k}_1), \tilde{w}(\mathbf{k}_2), \dots$ . However, only certain kinds of spatial nonlinearities can generate relative spatial phase information which is both nonredundant with the amplitude information and independent of absolute spatial position (and thus of potential relevance to object identification). A spatial shift by an amount  $\Delta\mathbf{x}$  will multiply the product  $\tilde{w}(\mathbf{k}_1)\tilde{w}(\mathbf{k}_2)\dots\tilde{w}(\mathbf{k}_n)$  by the product of the phase factors which correspond to the individual Fourier components:  $e^{i\mathbf{k}_1\Delta\mathbf{x}}e^{i\mathbf{k}_2\Delta\mathbf{x}}\dots e^{i\mathbf{k}_n\Delta\mathbf{x}}$ . In order for the value of this product to be independent of the spatial shift  $\Delta\mathbf{x}$ , the spatial frequencies must sum to zero:  $\mathbf{k}_1 + \mathbf{k}_2 + \dots + \mathbf{k}_n = 0$ . In the (trivial) case in which the number of components  $n$  is 1, this condition reduces to  $\mathbf{k}_1 = 0$ , which corresponds to the fact that the zero-frequency component (0) (the space-averaged luminance) is the only one whose phase is independent of absolute position. When the number of components  $n$  is 2, the sum-to-zero condition reduces to  $\mathbf{k}_2 = -\mathbf{k}_1$ . This corresponds to extraction of Fourier amplitudes, since  $\tilde{w}(\mathbf{k}_1)\tilde{w}(-\mathbf{k}_1) = |\tilde{w}(\mathbf{k}_1)|^2$ . That is, second-order interactions of spatial phases do not lead to any position-invariant terms that could not be obtained from analysis of the individual Fourier amplitudes. Only when the number of Fourier components  $n$  is three or more can such interactions provide new information. This is because it is possible to identify three or more spatial frequencies  $\mathbf{k}_1, \mathbf{k}_2, \mathbf{k}_3, \dots$  which sum to zero but do not consist of complex-conjugate pairs. The unique feature of the  $n \geq 3$ -cases (in comparison with the familiar  $n = 1$ - and  $n = 2$ -cases) is that they allow for position-independent quantities  $\tilde{w}(\mathbf{k}_1)\tilde{w}(\mathbf{k}_2)\dots\tilde{w}(\mathbf{k}_n)$  which are sensitive to the *relative* phases of several individual Fourier components.

The term  $\tilde{w}(\mathbf{k}_1)\tilde{w}(\mathbf{k}_2)\dots\tilde{w}(\mathbf{k}_n)$  may be independent of the relative phase of its factors, even for  $n \geq 3$ , if the frequencies  $\mathbf{k}_1, \mathbf{k}_2, \dots, \mathbf{k}_n$  consist of pairs of conjugate

frequencies  $\mathbf{k}_r$  and  $-\mathbf{k}_r$ , possibly along with occurrences of the 0-frequency. In this case, the interaction term  $\tilde{w}(\mathbf{k}_1)\tilde{w}(\mathbf{k}_2)\dots\tilde{w}(\mathbf{k}_n)$  reduces to a product of Fourier amplitudes. Such terms would dominate in models which depended on interactions between the energy in two spatial frequency channels, on a *nonquadratic* computation of energy within a single channel, or on the deviation of the power spectrum of texture samples from that of their ensemble.

The dependence on relative phase properly formalizes the essence of the local vs global distinction. Independence of relative phase is equivalent to computations based on global Fourier amplitudes, no matter what kinds of nonlinearities are applied. Fourier amplitudes are the phase-independent (i.e. position-independent) quantities that can be extracted from an array of receptive fields whose profiles are full-field gratings. Whether these Fourier amplitudes are processed independently or interact, such computations represent the extreme of global analysis.

A real receptive field is not likely to resemble a full-field grating, but will have some limited spread (and consequently, will be sensitive to more than a single spatial frequency). The output of a realistic receptive field may nevertheless be used in a global or a local fashion. One can imagine that spatial pooling of randomly positioned homologous receptive fields occurs in a fundamentally linear fashion. Because of the randomness of the receptive fields' positions, this will produce signals that are independent of the relative spatial phases in the stimulus—and is thus an implementation of a global analysis with local receptive fields. However, if such locally generated signals *interact nonlinearly prior to spatial pooling*—the essence of a local model—any further computations will contain traces of dependence on relative spatial phase.

There is another way to see that for a nonlinear receptive field with a linear front end, sensitivity to relative spatial phase implies local processing. Insensitivity to spatial phase would imply that all interaction terms  $\tilde{w}(\mathbf{k}_1)\tilde{w}(\mathbf{k}_2)\dots\tilde{w}(\mathbf{k}_n)$  consisted only of pairs of conjugate frequencies  $\mathbf{k}_r$  and  $-\mathbf{k}_r$ . That is, such terms cannot be accompanied by interaction terms  $\tilde{w}(\mathbf{k}_1 + \Delta\mathbf{k}_1)\tilde{w}(\mathbf{k}_2 + \Delta\mathbf{k}_2)\dots\tilde{w}(\mathbf{k}_n + \Delta\mathbf{k}_n)$  at nearby, but unpaired, spatial frequencies. Therefore, a high degree of spatial frequency selectivity is necessary to allow interactions among a set of spatial frequencies,  $\mathbf{k}_1, \mathbf{k}_2, \dots, \mathbf{k}_n$  but not among nearby spatial frequencies  $\mathbf{k}_1 + \Delta\mathbf{k}_1, \mathbf{k}_2 + \Delta\mathbf{k}_2, \dots, \mathbf{k}_n + \Delta\mathbf{k}_n$ . As is well known (Daugman, 1985), the frequency selectivity (bandwidth) is reciprocally related to the summing length. That is, insensitivity to relative spatial phase (exclusion of interactions among nonconjugate spatial frequencies) requires a high degree of frequency selectivity, which in turn requires a large summing area. Conversely, small summing areas provide the opportunity for interactions across a range of spatial frequencies, and thus allows simple nonlinearities to generate generic terms

$\tilde{w}(k_1)\tilde{w}(k_2)\dots\tilde{w}(k_n)$  that depend on relative spatial phases.

#### *Implications of the dependence of responses on spatial phase*

In this study, we have shown that responses to certain textures depend strongly on spatial phase, and thus, that the neural computations underlying the generation of the VEP are fundamentally local, in the sense we have formalized above. This conclusion relies only on a comparison of responses to textures with undistorted spatial phases ( $\theta = 0$ ) to textures in which spatial phases have been completely randomized ( $\theta = \pi$ ). However, we have also examined responses parametric in the degree of randomization ( $\theta$ ). A straightforward but tedious calculation shows that for the even textures, there is an asymptotic limit (check sizes larger than receptive field elements) in which the dependence of interactions on the amount of spatial phase randomization is approximately  $[(\sin \theta)/\theta]^4$ . This function has a value of 1 at  $\theta = 0$  and declines rapidly over the range  $[0, \pi]$ , achieving a value of 0.16 at  $\theta = 0.5\pi$ . In view of the approximations made to derive the expression, we expect that it will be valid for responses to stimuli with sufficiently large check sizes, but that, (as check size decreases below some critical value) departures from this behavior will occur. When checks are sufficiently small, we anticipate that responses will not decline to zero even for  $\theta = \pi$ , because of conjugate-frequency terms originating in pointwise nonlinearities. This is consistent with our results (Fig. 4), in which the antisymmetric response size has the dependence  $[(\sin \theta)/\theta]^4$  on check size for 8 and 16 min checks, but does not decline to zero for checks of size 4 min.

#### *Implications for modeling of the genesis of the antisymmetric response component*

Since isodipole texture pairs have, in an ensemble sense, the same spatial frequency content, discrimination between them necessarily relies on processing beyond linear filtering and extraction of power spectra. Thus, studies of visual discriminations between isodipole textures (Caelli & Julesz, 1978; Julesz *et al.*, 1978, Victor, 1985) represent a probe to analyze nonlinear mechanisms underlying the extraction of local features. However, despite the equality of second-order statistics at the ensemble level, individual *instances* of isodipole textures necessarily differ in spectral content. In principle, these differences might support isodipole texture discrimination based on *global* power spectral statistics [see discussion in Yellott (1993) and Victor (1994)]. The present study forces rejection of this hypothesis. Whatever inter-example differences in global power spectra might be present in individual examples are preserved by spatial phase jittering. Nevertheless, spatial phase jitters of  $>0.5\pi$  radians destroyed the distinguishing features of the isodipole textures, and the associated antisymmetric VEP component. This implies that local features, not global spectral content, underlie

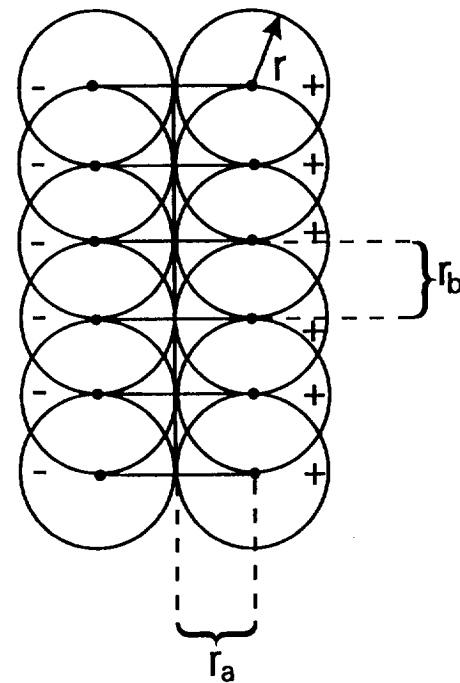


FIGURE 9. Proposed model for the generation of the antisymmetric response by even textures. The local subunits are antagonistic Gaussians of radius  $r$  separated by an amount  $2r_a$ . Their outputs are rectified, and rectified signals pooled from  $N$  collinear subunits (each separated by an amount  $r_b$ ) are subject to a threshold  $h$ .

the difference in processing of distinguishable isodipole textures.

Previously (Victor & Conte, 1989, 1991), we have used the dependence of the antisymmetric response on texture type and degree of correlation to construct a local computational model (Fig. 9) for edge extraction. The essential features of this model (Fig. 7 of Victor & Conte, 1991) are: (i) local subunits whose outputs are independently rectified; and (ii) a second nonlinearity which pools these outputs along a line. Elimination of either of the two nonlinearities collapses the model to more standard models of cortical cells and edge detectors, but fails to account for the antisymmetric response component. With both nonlinearities intact and at least four subunits, this model accounted for which classes of fourth-order isodipole textures are distinguishable psychophysically, and for the dependence of the size of the antisymmetric response on short- and long-range correlations (Victor & Conte, 1989). Furthermore, the distinctive dynamics of the antisymmetric VEP response to the triangle textures (which are third-order isodipole textures) suggested that these textures generate an antisymmetric response via a different mechanism (Victor & Conte, 1991), and were not accounted for by this model.

We now examine this model's response to the phase-jittered even textures via Monte Carlo simulations, with model parameters taken from Table 6 of Victor and Conte (1991):

$N$  (number of subunits)—6;

$h$  (strength of second nonlinearity)—0.6;

$r$  (radius of subunit Gaussian)— $0.5 \times$  check size;

$r_a$  (separation of Gaussians within subunit)— $0.5 \times$  check size;

$r_b$  (separation of subunits)— $0.5 \times$  check size.

To generate responses from this model, the computational units shown in Fig. 9 were placed in random position and orientation on examples of the even and random textures. For each placement, the output of each computational unit was calculated as described more fully in Victor and Conte (1991): linear summation within each Gaussian, subtraction of responses within each edge detector pair, rectification of this "subunit" response, summation of subunit responses, and a final threshold. This procedure was carried out for 100 random placements of the computational unit on 100 examples of each texture. The predicted "antisymmetric response" was equal to the difference between the average output generated in response to the even texture and the average output generated in response to the random texture. Across the range of phase jittering used in these experiments, the model's antisymmetric response closely matches the asymptotic prediction  $[\sin(\theta)/(\theta)]^4$  experimentally observed behavior for 8 and 16 min checks (Fig. 4).

Previously (Victor & Conte, 1989), we demonstrated an approximate proportionality between the size of the computational unit which generates the antisymmetric response, and the check size of the stimulus, and showed that this scaling was not due to retinotopic variation of receptive field size. In order to account for this scaling, we postulated that the basic computational unit is present across a range of spatial scales [see also Purpura *et al.*, (1994)]. Since units with summing areas that are either substantially smaller or substantially larger than the check size do not contribute significantly to the response, only those units with check sizes which are well-matched to the check size need to be considered. Empirically (Fig. 8 of Victor & Conte, 1989), this scaling behavior breaks down for checks of size 4 min or smaller. Correspondingly, Monte Carlo simulations based on computational units which were twice as large (relative to the check size) as those used for the 8 and 16 min checks correctly predict that response size declines with phase jitter, but not to zero. Another feature of the present data is that although perturbation of phases via the product method destroys all pairwise and third-order correlations among Fourier components, the antisymmetric response to the even textures is preserved. This too is predicted by the Monte Carlo simulations.

#### *Relevance for contrast gain control*

It is well recognized that some kind of adjustment of responsiveness based on a neural measure of contrast is both a widespread feature of cortical neurons, as well as crucial for efficient extraction of local features (Heeger, 1992). Our model (Fig. 9) represents an elaboration of standard models for edge detection, in which two spatial nonlinearities combine to form a computational unit

which extracts edges independent of changes in the sign of contrast. For this computational unit to retain its specificity over a wide contrast range, it is necessary that the effective setpoint of the second nonlinearity be adjusted based on some measure of stimulus contrast. Otherwise, setpoints which sufficed to detect edges at low contrasts would lose specificity at high contrasts, or setpoints which provided adequate specificity at high contrasts would fail to detect edges at low contrasts.

Phase jittering dissociates the salience of local features from contrast, and thus provides a means to determine whether the neural measure of contrast and the extraction of local features are related in a feedback or feedforward fashion. As seen in Figs 5 and 6, increases in contrast result in a phase advance, but only slight enhancements in the amplitude of the symmetric and antisymmetric response components. However, phase jitter reduces antisymmetric response size, without retarding the response phase. This implies that the neural measure of contrast is derived prior to the extraction of local features. That is, the gain control appears to act in a feedforward manner, in which contrast (independent of the presence or absence of local features) adjusts the gain and dynamics of a feature-extraction stage. Had the gain control been feedback, then increasing phase jitter (and reduced antisymmetric response size) would have been associated with an additional phase lag.

#### *Relationship to other studies of spatial phase*

Although the most dramatic evidence that spatial phase conveys information which is crucial to object identification is derived from studies of natural images (Oppenheim & Lim, 1981; Field, 1987; Shapley *et al.*, 1990; Morgan *et al.*, 1991), most quantitative analyses of the role of spatial phase have been restricted to stimuli which vary along a single dimension. Successful models of detection of one-dimensional patterns [see Graham (1989) for an overview] require channels of relatively broad bandwidth (i.e. local filters), which interact by probability summation (Wilson & Bergen, 1979). Such models necessarily result in at least a subtle sensitivity to spatial phase. As shown by Nachmias (1993), even detection of single sine gratings amidst visual noise cannot be accounted for simply on the basis of spatial frequency content. This was interpreted in terms of a local model (Green, 1983), which again implies a role for spatial phase.

Several investigators have identified sensitivity to relative spatial phase in discrimination among one-dimensional periodic luminance (Nachmias & Weber, 1975; Burr, 1980; Badcock, 1984a, b) and chromatic (Girard & Morrone, 1995) patterns. The studies of Rentschler and Treutwein (1985), Bennett and Banks (1987), and Morrone *et al.* (1989) provide strong direct evidence for foveal sensitivity to the relative phase of gratings, although they differed as to whether peripheral discrimination of spatial phase is intrinsically inferior to that of the fovea. Morrone and Burr (1988) demonstrated that manipulation of the relative phases of the Fourier

components of square waves and related stimuli played a crucial role in the appearance of features such as edges, and proposed a model which relied on phase relationships between broadly tuned (i.e. local) spatial filters. Regan and Regan (1988) used a VEP approach to examine interactions between pairs of vertical sine gratings, each of which were modulated by independent frequencies. Although some of the interaction terms (e.g.  $2F_1 + 2F_2$ ) were independent of spatial phase, others (e.g.  $F_1 + F_2$ ,  $F_1 + 3F_2$ , and  $5F_2 - F_2$ ) were strongly dependent on spatial phase.

In studies of stimuli which vary along two dimensions, Georgeson and Shkelton (1994) showed that the amount of energy at one orientation can influence the perceived contrast at a second orientation, but did not determine whether this interaction was dependent on spatial phase. Other recent studies have shown that spatial phase played a role both in the detection and apparent contrast (Tiippana *et al.*, 1994) of compound two-dimensional grating patterns. Julesz' studies of isodipole textures (Caelli & Julesz, 1978; Julesz *et al.*, 1978; Julesz, 1981), which demonstrate perceptual differences in textures despite similar spectral content, imply (see above) that the perception of local features depends either on high-order moments of Fourier amplitudes or on phase-dependent interactions among several spatial frequencies. In this study, by explicitly examining the role of spatial phase in isodipole textures, we have eliminated the role of high-order moments of Fourier amplitudes, and thus demonstrated the importance of spatial phase.

One difficulty with the interpretation of many of these studies is that alteration of the spatial phases of the components of a compound grating necessarily changes its intensity profile. For one-dimensional patterns, sensitivity to relative contrasts within this profile suffice to account for spatial phase discrimination (Badcock, 1984a, b), and thus there appears to be no need to postulate mechanisms sensitive to spatial phase *per se*. For two-dimensional patterns, this argument is less compelling, because the superposition of a grating in a second direction will tend to mask differences in intensity profile. While we agree that a local analysis (Victor & Conte, 1991), rather than sensitivity to spatial phase *per se*, is the likely basis for our findings, it is important to note that sensitivity to differences in the intensity profile cannot account for discrimination among isodipole textures either. Unblurred isodipole textures have the identical intensity profile, and blurred, phase jittered textures have intensity profiles which are very nearly Gaussian and have identical variance.

Interpreted in the context of Fourier analysis, the interactions required to account for our results would involve specific interactions among four (or more) spatial frequencies in separate directions. The need for a four-way multiplication or equivalent process makes models based on narrow-band filters physiologically untenable. Rather, along with Morrone and Burr (1988), we interpret these findings in terms of a local model whose filters are broadly tuned in the frequency domain (Victor & Conte,

1991), rather than as indicative of processing driven by spatial phase combinations of high order.

### Summary

In conclusion, by manipulating the relative phases of spatial Fourier components, we have shown that the nonlinear processes involved in texture discrimination cannot be accounted for on the basis of the global characteristics of their spatial frequency spectrum. Generic phase decorrelations eliminate the VEP measures of texture discrimination, but phase manipulations which destroy all pairwise and third-order correlations yet retain certain higher-order correlations preserve the antisymmetric VEP response to even textures. These findings are accounted for by a computational unit which contains rectification within a subunit, and nonlinear combination of subunit signals across a wider range. The modulatory effect of contrast on response size and timing (temporal phase) appears to be mediated by a feedforward process which is insensitive to spatial phase.

### REFERENCES

- Badcock, D. R. (1984a). Spatial phase or luminance profile discrimination? *Vision Research*, 24, 613–623.
- Badcock, D. R. (1984b). How do we discriminate relative spatial phase? *Vision Research*, 24, 1847–1857.
- Bennett, P.J. & Banks, M. S. (1987). Sensitivity loss in odd-symmetric mechanisms and phase anomalies in peripheral vision. *Nature*, 326, 873–876.
- Burr, D. C. (1980). Sensitivity to spatial phase. *Vision Research*, 20, 391–396.
- Caelli, T. & Julesz, B. (1978). On perceptual analyzers underlying visual texture discrimination. Part I. *Biological Cybernetics*, 28, 167–175.
- Campbell, F. W. & Green, D. C. (1965). Optical and retinal factors affecting visual resolution. *Journal of Physiology*, 181, 576–593.
- Daugman, J. G. (1985). Uncertainty relations for resolution in space, spatial frequency and orientation optimized by two-dimensional visual cortical filters. *Journal of the Optical Society of America*, A2, 1160–1169.
- Dobie, R. A. & Wilson, M. J. (1993). Objective response detection in the frequency domain. *Electroencephalography and Clinical Neurophysiology*, 88, 516–524.
- Field, D. (1987). Relations between the statistics of natural images and the response properties of cortical cells. *Journal of the Optical Society of America*, A4, 2379–2394.
- Georgeson, M. A. & Shkelton, T. M. (1994). Perceived contrast of gratings and plaids: Non-linear summation across oriented filters. *Vision Research*, 34, 1061–1075.
- Girard, P. & Morrone, M. C. (1995). Spatial structure of chromatically opponent receptive fields in the human visual system. *Visual Neuroscience*, 12, 103–116.
- Graham, N. V.S. (1989). *Visual pattern analyzers*. Oxford: Clarendon Press.
- Green, D. M. (1983). Profile analysis. *American Psychology*, 38, 133–142.
- Heeger, D. J. (1992). Normalization of cell responses in cat striate cortex. *Visual Neuroscience*, 9, 181–197.
- Julesz, B. (1981). Textons, the elements of texture perception, and their interactions. *Nature*, 290, 91–97.
- Julesz, B., Gilbert, E. N. & Victor, J. D. (1978). Visual discrimination of textures with identical third-order statistics. *Biological Cybernetics*, 31, 137–149.
- Kelly, D. H. (1972). Adaptation effects on spatio-temporal sine wave thresholds. *Vision Research*, 12, 89–102.
- Milkman, N., Schick, G., Rossetto, M., Ratliff, F., Shapley, R. &



- Victor, J. D. (1980). A two-dimensional computer-controlled visual stimulator. *Behavioral Research Methods and Instrumentation*, 12, 283–292.
- Morgan, M. J., Ross, J. & Hayes, A. (1991). The relative importance of local phase and local amplitude in patchwise image reconstruction. *Biological Cybernetics*, 65, 113–119.
- Morrone, M. C. & Burr, D. C. (1988). Feature detection in human vision: A phase-dependent energy model. *Proceedings of the Royal Society of London*, 235, 221–245.
- Morrone, M. C., Burr, D. C. & Spinelli, D. (1989). Discrimination of spatial phase in central and peripheral vision. *Vision Research*, 29, 433–435.
- Nachmias, J. (1993). Masked detection of gratings: The standard model revisited. *Vision Research*, 33, 1359–1365.
- Nachmias, J. & Weber, A. (1975). Discrimination of simple and complex gratings. *Vision Research*, 15, 217–223.
- Oppenheim, A. V. & Lim, J. S. (1981). The importance of phase in signals. *Proceedings of the IEEE*, 69, 529–541.
- Purpura, K., Victor, J. D. & Katz, E. (1994). Striate cortex extracts higher-order spatial correlations from visual textures. *Proceedings of the National Academy of Science USA*, 91, 8482–8486.
- Regan, D. & Regan, M. P. (1988). Objective evidence for phase-independent spatial frequency analysis in the human visual pathway. *Vision Research*, 28, 187–191.
- Rentschler, I. & Treutwein, B. (1985). Loss of spatial phase relationships in extrafoveal vision. *Nature*, 313, 308–310.
- Shapley, R., Caelli, T., Grossberg, S., Morgan, M. J. & Rentschler, I. (1990). Computational theories of visual perception. In Spillman, L. & Werner, J. B. (eds). *Visual perception: the neurophysiological foundations* (pp. 417–447). New York: Academic Press.
- Tadmor, Y. & Tolhurst, D. J. (1992). Both the phase and the amplitude spectrum may determine the appearance of natural images. *Vision Research*, 31, 141–145.
- Tiippana, K., Näsänen, R. & Rovamo, J. (1994). Contrast matching of two-dimensional compound gratings. *Vision Research*, 34, 1157–1163.
- Victor, J. D. (1985). Complex visual textures as a tool for studying the VEP. *Vision Research*, 25, 1811–1827.
- Victor, J. D. (1994). Images, statistics, and textures: A comment on “Implications of triple correlation uniqueness for texture statistics and the Julesz conjecture”. *Journal of the Optical Society of America*, A11, 1680–1684.
- Victor, J. D. & Conte, M. M. (1987). Local and long-range interactions in pattern processing. *Investigative Ophthalmology and Visual Science*, 28 (suppl.) 362.
- Victor, J. D. & Conte, M. M. (1989). Cortical interactions in texture processing: Scale and dynamics. *Visual Neuroscience*, 2, 297–313.
- Victor, J. D. & Conte, M. M. (1991). Spatial organization of nonlinear interactions in form perception. *Vision Research*, 31, 1457–1488.
- Victor, J. D. & Mast, J. (1991). A new statistic for steady-state evoked potentials. *Electroencephalography and Clinical Neurophysiology*, 78, 378–388.
- Victor, J. D. & Zemon, V. (1985). The human visual evoked potential: Analysis of components due to elementary and complex aspects of form. *Vision Research*, 25, 1829–1844.
- Wilson, H. R. & Bergen (1979). A four mechanism model for threshold spatial vision. *Vision Research*, 19, 19–32.
- Yellott, J. (1993). Implications of triple correlation uniqueness for texture statistics and the Julesz conjecture. *Journal of the Optical Society of America*, A10, 777–793.

---

*Acknowledgements*—A portion of this work was presented at the 1993 meeting of the Association for Research in Vision and Ophthalmology in Sarasota, Florida. This work was supported by NIH Grant EY7977 and The Hirschl Trust.